

Effect of annealing process in water on the essential work of fracture response of ultra high molecular weight polyethylene

Sinan Yilmaz · Taner Yilmaz · A. Armagan Arici

Received: 8 July 2010/Accepted: 8 October 2010/Published online: 22 October 2010
© Springer Science+Business Media, LLC 2010

Abstract The toughness of ultra high molecular weight polyethylene (UHMWPE) before and after annealing process in water was investigated by the essential work of fracture (EWF) method. Annealing in water at 80 °C for various aging periods of the 5 mm thickness with various ligament lengths single edge notched tension (SENT) specimens was performed in hot water. Tensile tests were performed at 2 mm/min constant deformation rate at room temperature in order to determine EWF parameters. After tensile tests, the fracture cross-sections of SENT specimens were investigated by scanning electron microscope (SEM). From the 60th day of annealing process in water, it was seen that the fracture toughness of the material decreased while water absorption in samples increased.

Introduction

Thermoplastic polymers are widely used in engineering due to their beneficial properties but the quality of the thermoplastic product changes during service. Property degradation owing to annealing in water may be a severe constraint for the targeted application. That is the reason why great efforts are devoted to the stabilization of thermoplastics,

especially for those which are sensitive to environmental influences. It is known that annealing in water manifests first in a color change without noticeable effect on the mechanical properties. Progressing annealing results later in substantial deterioration of the mechanical characteristics that is well reflected by the toughness response. Changes in the toughness of polymers can well be followed by concepts of the fracture mechanics. Note that a suitable fracture mechanical method yields a material parameter which does not depend on the specimen type and dimension [1, 2].

It is well established that when failure of notched specimens is brittle in nature, the area in which energy is dissipated near the crack tip is so small that the entire specimen can be assumed to exhibit Hookean elasticity. This type of failure can be studied using linear elastic fracture mechanics (LEFM) [3]. The critical stress intensity factor (K_{Ic}) and critical strain energy release rate (G_{Ic}) proved to be material constants under certain testing conditions that ensure small scale yielding in the specimens. However, this approach cannot be adopted for toughened polymers which exhibit gross yielding during fracture. For the assessment of the fracture toughness of such ductile polymers, the essential work of fracture (EWF) method is gaining acceptance due to its experimental simplicity [4]. The EWF assumes that the non-elastic region at the tip of a crack may be divided into two regions: an inner region where the fracture process takes place, and the outer region where the plastic deformation takes place. The total work of fracture can then be partitioned into two components: work that is expended in the inner fracture process zone (IFPZ) to form a neck and subsequent tearing, and the work which is consumed by various deformation mechanisms in the surrounding outer plastic deformation zone (OPDZ). The former is referred to as “Essential Work of Fracture” and the latter as “Non-Essential Work of Fracture” [5, 7].

S. Yilmaz · A. Armagan Arici
Department of Mechanical Engineering, Kocaeli University,
Umuttepe, 41380 Izmit, Turkey

T. Yilmaz (✉)
Civil Aviation College, Kocaeli University, Arslanbey Campus,
41285 Izmit, Turkey
e-mail: taner.yilmaz@kocaeli.edu.tr

T. Yilmaz
Natural and Applied Sciences, Kocaeli University,
Umuttepe Campus, 41380 Izmit, Turkey

In this study, EWF approach was used to determine the fracture toughness of ultra high molecular weight polyethylene (UHMWPE) before and after annealing process in water. Annealing in water was performed in hot water at 80 °C for 90 days.

EWF

EWF approach, first developed by Broberg [1] is based on the assumption that the total work of fracture, W_f is the sum of two energy terms,

$$W_f = W_e + W_p \quad (1)$$

where the first term, W_e , is the EWF, which is the energy consumed in the IFPZ, where the actual fracture occurs (see Fig. 1). W_e is therefore a pure crack resistance parameter and thus regarded as fracture toughness. The second term, W_p , which is referred to as the non-essential work or plastic deformation work, is the energy dissipated in the OPDZ as shown in Fig. 1, which for polymers involves microvoiding and shear yielding [7].

When both the IFPZ and the OPDZ contained in the ligament, then W_e is proportional to the ligament length, L and W_p is proportional the square of the ligament length L^2 . Hence it can be written as:

$$W_e = w_e TL \quad (2)$$

$$W_p = \beta w_p TL^2 \quad (3)$$

where w_e is termed the specific EWF and βw_p is termed the specific non-EWF. The parameter β is proportionality

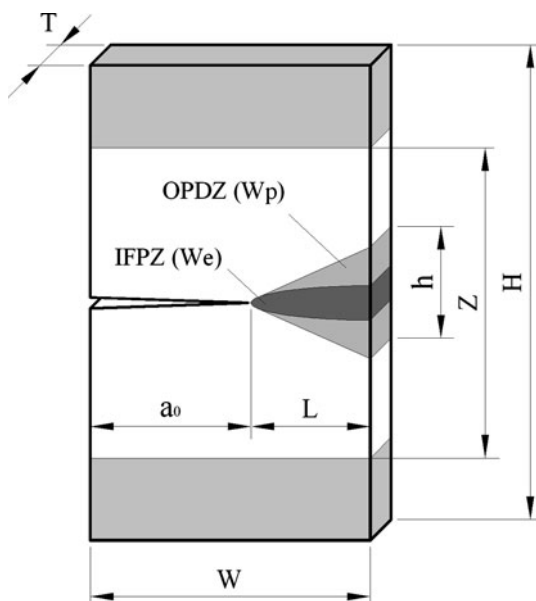


Fig. 1 Inner fracture process zone (IFPZ) and outer plastic deformation zone (OPDZ) in a single edge notched tension (SENT) specimen

constant (plastic zone shape factor) whose value depends on the geometry of the specimen and the crack [4] but it is independent of the ligament length, we obtain:

$$w_f = w_e + \beta w_p L \quad (4)$$

where w_e is termed the “Specific Essential Work of Fracture (SEWF)”, w_p is termed the “Specific Non-Essential Work of Fracture (SNEWF)”, and w_f is the specific total work of fracture.

To verify how the state of stress may depend on ligament length, values of the maximum net-section stress, $\sigma_n = \frac{P_{\max}}{L^2}$ (where P_{\max} is the maximum load on the load-displacement curve) are often plotted against ligament length, L . Under pure plane stress conditions $\sigma_n = m\sigma_y$ where m is the plastic constraint factor whose value for single edge notched tension (SENT) specimen is 1.0 and for DENT specimen is 1.15. The value of m increases with the decreasing ligament length [7, 8].

It is also possible to distinguish between the specific work of fracture for yielding (w_y) and the specific work of fracture for necking and subsequent fracture (w_{nt}). The specific total work of fracture, w_f may thus be written as:

$$w_f = w_e + \beta w_p L = w_y + w_{nt} \quad (5)$$

When W_f is partitioned in this way, variation of the specific work terms w_y and w_{nt} with L follows that of w_f with L . Equation 3 was then split into:

$$w_y = w_{e,y} + \beta_y w_{p,y} L \quad (6)$$

$$w_{nt} = w_{e,nt} + \beta_{nt} w_{p,nt} L \quad (7)$$

where the terms $w_{e,y}$ and $w_{e,nt}$ represent the yielding and the necking/tearing components of the specific EWF, respectively [9, 10].

The crack opening displacement can be obtained by plotting the extension at break, e_b , versus ligament length. Variation of e_b with L conforms to a straight-line relationship of the form:

$$e_b = e_0 + e_p L \quad (8)$$

where e_0 is the intercept value of e_b at zero ligament length representing the COD (crack opening displacement) of the advancing crack tip and e_p is the plastic contribution to extension [11].

Experimental details

A UHMWPE [12] sheet, having 800 × 500 × 5 mm dimensions was used in this study. From that sheet, 78 rectangular coupons having width (W) of 35 mm and length (H) of 110 mm were prepared. The length of the coupon was always perpendicular to the long edge of the sheet. The coupons were then notched to produce series of

Table 1 Annealing time in water and geometric parameters of SENT samples

Annealing time (days)	<i>L</i> (mm)	<i>W</i> (mm)	<i>H</i> (mm)	<i>T</i> (mm)	<i>Z</i> (mm)
1, 3, 7, 15, 30, 60, 90	3, 5, 7, 10, 15, 20, 25	35	110	5	70

SENT specimens as shown in Fig. 1 with ligament length (*L*) ranging from 3 to 25 mm. Having prepared SENT type specimens were immersed in water at 80 °C and kept for various aging periods (Table 1). Fracture surface analysis on the SENT was also performed to determine the mechanisms of failure. These fractographic examinations were done using a JEOL JSM M-6060, after depositing a gold layer on the fracture surfaces by ion sputtering.

In the case of fracture tests, for each ligament length, three specimens were fractured in an Instron 4411 universal testing device at 2 mm/min constant deformation rate at room temperature.

From the recorded load–displacement curves, the following parameters were evaluated and their variations with respect to ligament length, *L* were studied:

- Net-section stress at maximum load, $\sigma_n = \frac{P_{\max}}{LT}$
- Extension to break, $e_b = e_0 + e_p L$
- Specific total work of fracture, $w_f = W_f/LT$
- Specific work of fracture for yielding, $w_y = W_y/LT$
- Specific work of fracture for subsequent tearing, $w_{nt} = w_f - w_y$

Results and discussions

As-received UHMWPE

Figure 2 shows typical F–x curves of the SENT specimens at various ligament lengths. These curves indicate that SENT specimens fail by ductile tearing of the ligament region. However, there was no evidence of load-drop at maximum load [13–16] in any of the SENT curves obtained in this study as in previous studies [5–7].

The notable feature of the curves as a function of ligament length is their geometrical similarity, which is an essential pre-requisite for EWF testing. This observation as well as the contraction of specimen surfaces suggested that crack propagation in these specimens occurred under plane stress conditions [3, 17, 18].

The EWF (w_e) was read from the intercept of the linear regression line with the ordinate. Figure 3a also contains the slope value and the correlation coefficient of the related regression line. The well-marked yielding in the F–x curves of UHMWPE allows us to distinguish between the specific work of fracture required for yielding (w_y) and that consumed by tearing and fracture (w_n) [10]. Figure 3a shows

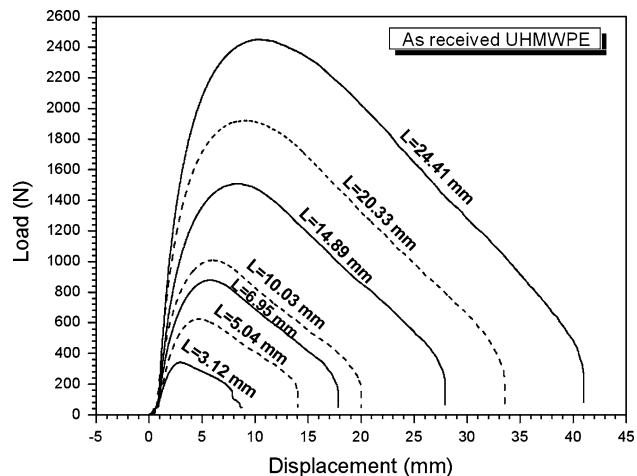


Fig. 2 Typical load–displacement diagrams for SENT specimens at room temperature for various ligament lengths, *L*

plots of the specific work of fracture parameters, w_f , w_y , and w_{nt} versus ligament length, *L*, for as-received material. It can be seen from these plots that for the range of ligament lengths used here, variation of w_f , w_y , and w_{nt} with *L* is indeed linear. Figure 3 also shows plots of net-section stress and extension to break versus ligament length. As it can be seen from the plot, variation of e_b is also linear (Fig. 3c). It is seen from Fig. 3b, that σ_n decreases steadily with increasing *L*, reaching a steady state value (σ_{ns}), at large ligament lengths.

Another feature of Fig. 3b which is worthy of consideration, is the elevated values of σ_n at small ligament lengths. This behavior is often attributed to the change in the stress state in the ligament region because of a transition from a pure plane stress fracture to a mixed mode fracture [3, 7].

Annealed UHMWPE in water

The prerequisites of the EWF application were also satisfied after annealing process in water because of the geometrical similarity of the load–displacement curves. Figure 4a depicts the F–x curves of the SENT specimens before and after 90 days storage in hot water when tested at ambient temperature. Comparing F–x response of SENT specimens at as-received and 90th day of aging stages (Fig. 4a) a decrease on the absorbed energy after maximum load can be noticed. Until the maximum load, there is not any significant change on the curves in Fig. 4a. It can be

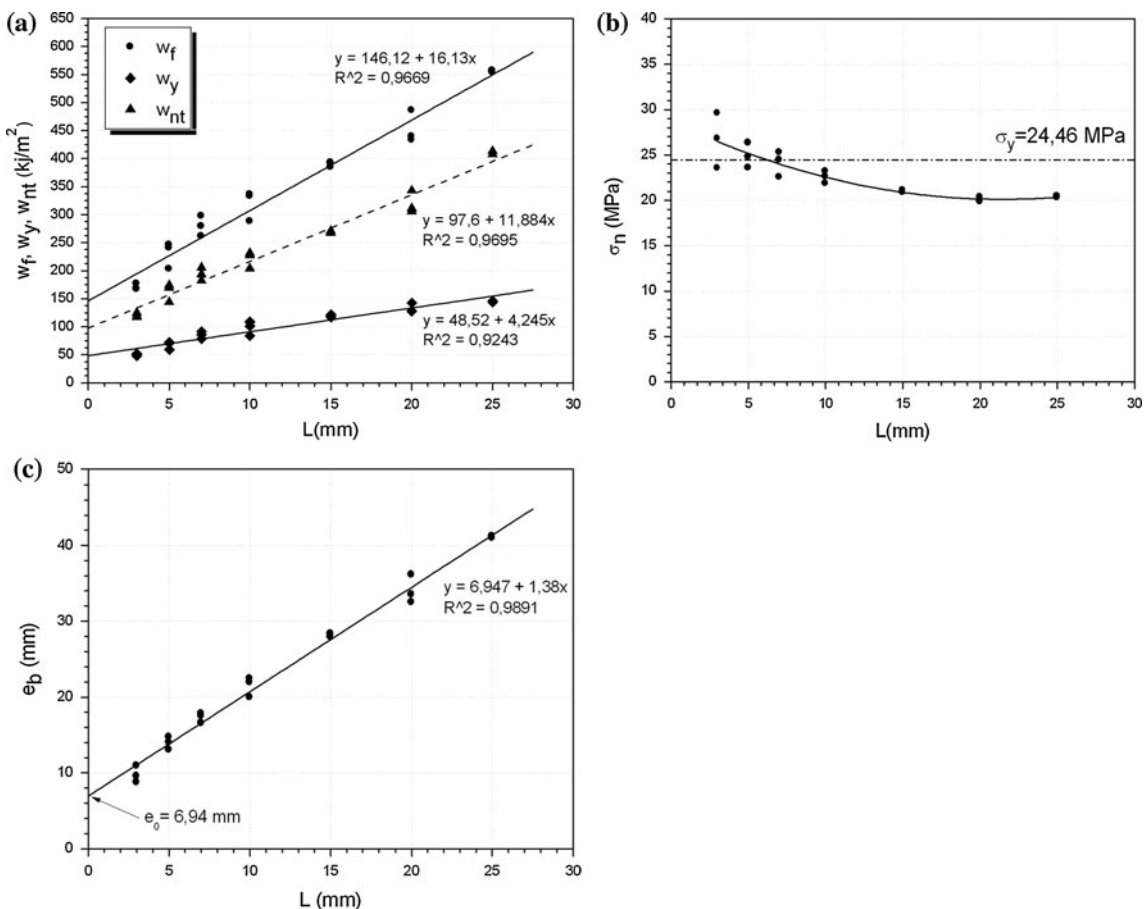


Fig. 3 **a** Specific work of fracture parameters versus ligament length, L , **b** net-section stress, σ_n and **c** extension to break, e_b , versus ligament length for as-received material

deduced from the curves that annealing process in water especially affected the work of plastic deformation. It can be seen from Fig. 4a that there is no load-drop at maximum load both for as-received material and 90th day material. So it cannot be confirmed if ligament region was fully yielded at maximum load. Nevertheless attention was paid to the maximum load registered on the load displacement curves [3, 7].

Figure 4b shows plots of the specific work of fracture parameters, w_f , w_y , and w_{nt} versus ligament length, L , for 90th day material. Variation of w_f , w_y , and w_{nt} with L is also linear as in as-received material but there is a significant difference between as-received material and 90th day material on EWF parameters (Table 2) due to annealing process.

To understand the effect of annealing process in water on the variation of net-section stress (σ_n) with ligament length (L), the plots of σ_n-L is given in Fig. 4c for as-received and for 90th day material. The prominent attribute of the figure is the variation of net-section stress with ligament length for 90th day material; there is not an

elevation on the values of σ_n at small ligament lengths because of the annealing effect. The crack tip plastic deformation zone of the annealed material did not enhance enough to disturbed by the lateral boundaries of the specimen and as a result of this the values of σ_n did not increase at small ligament lengths. In other words the state of the stress for 90 days annealed material in water is always pure plane stress. The net-section stress of annealed material for all ligament lengths is approximately equal yielding strength ($\approx \sigma_{y-90} = 23.3$ MPa).

The effect of annealing process in water on extension to break can be found in Fig. 4d. The extrapolated value (crack opening displacement value), e_0 is regressed from 6.94 to 5.30 mm for 90th day of annealing process in water. The variation of extension to break with ligament length is fairly linear for annealed material as in as-received material.

Figure 5 shows crack tip plastic deformation zone for as-received and 90th day samples. Notable feature of this figure is the shape and size of plastic deformation zones; for as-received samples size of the plastic deformation

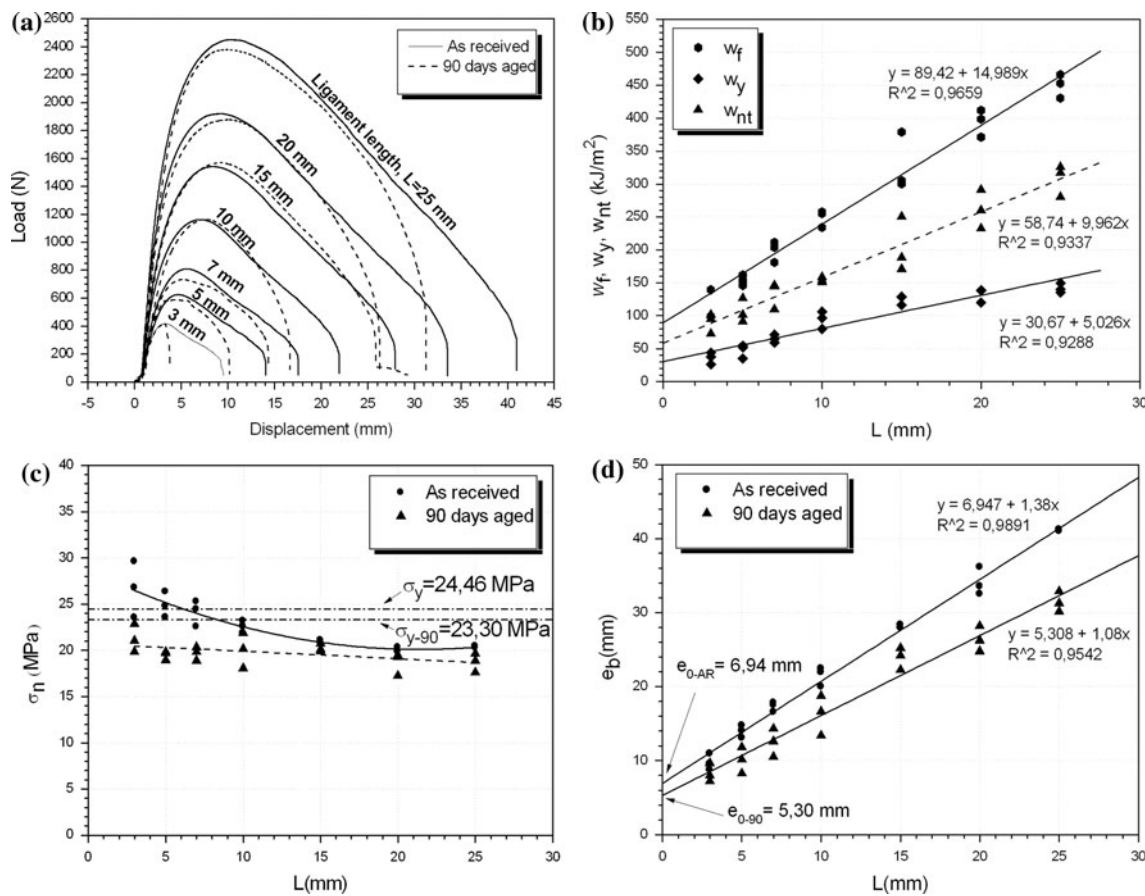


Fig. 4 **a** Comparison of the force–elongation curves of as-received and 90 days annealed SENT specimens for various ligament lengths. **b** Specific work of fracture parameters versus ligament length, L .

c Net-section stress, σ_n , **d** extension to break, e_b , versus ligament length for as-received and 90 days annealed material

Table 2 Work of fracture parameters for as-received and 90th day UHMWPE samples

Annealing period	EWF parameters					
	w_e (kJ/m ²)	βw_p (MJ/m ³)	$w_{e,y}$ (kJ/m ²)	$\beta_y w_{p,y}$ (MJ/m ³)	$w_{e,nt}$ (kJ/m ²)	$\beta_{nt} w_{p,nt}$ (MJ/m ³)
As-received	146.12	16.12	48.52	4.24	97.60	11.88
90th day	89.41	14.98	30.67	5.02	58.74	9.96

zone is increasing with increasing ligament length while the shape is almost same (geometrically similar) but for 90th day samples size of the plastic deformation zone is also increasing with increasing L but the shape of it is not similar for all ligament lengths because of the annealing effect.

From Fig. 6a and b, specific essential and plastic work terms were determined according to Eqs. 5 and 6. The related specific essential and plastic data are depicted as a function of the annealing time in Fig. 6c and d. One can notice that from the 60th day of the process annealing in water strongly reduces the specific EWF parameters. On

the other hand, the effect of annealing process is less pronounced for the specific plastic work terms (Fig. 6c, d). Plastic work was influenced by the water uptake and the water worked as plasticizer in UHMWPE [2].

Effect of annealing time in water

To understand the effect of annealing time on the fracture response of UHMWPE via examining the variations of thermal characteristics (degree of crystallinity and melting temperature), A Mettler Toledo DSC1 (differential scanning calorimetry) was used to measure the heat of fusion of

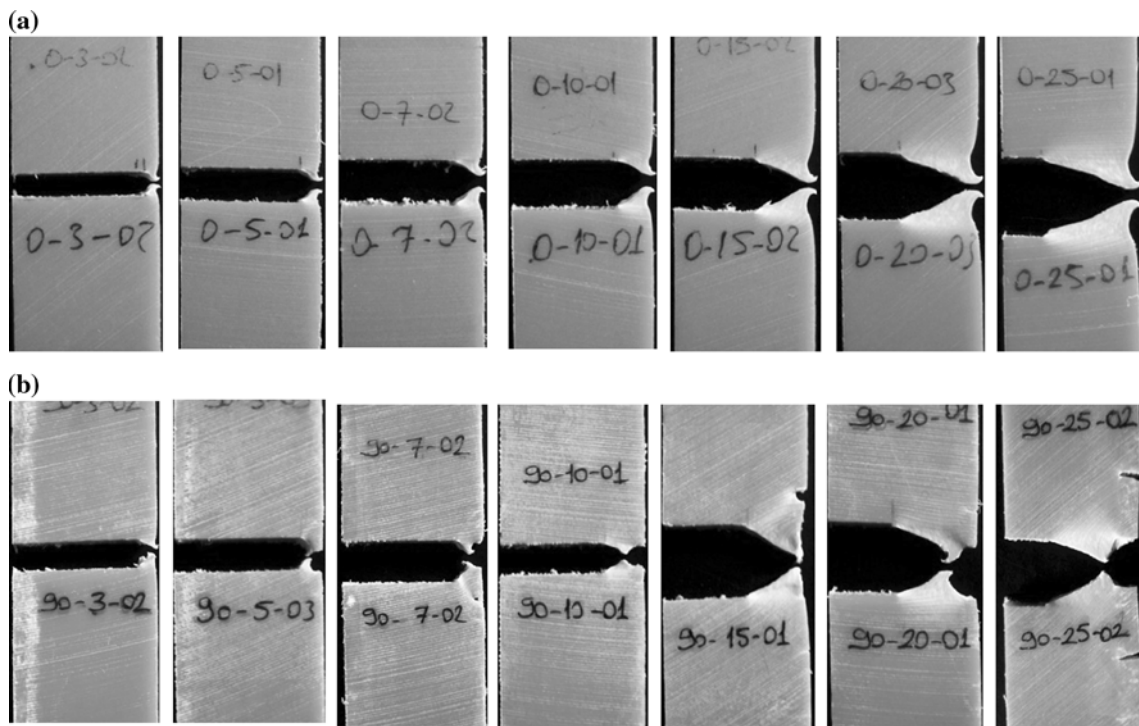


Fig. 5 Plastic deformation zones of **a** as-received and **b** 90 days annealed in water samples for various ligament lengths

the UHMWPE under nitrogen atmosphere. For this purpose the DSC analysis for 0, 15, 30, 60 and 90th days of annealing process in water was carried out between 30 and 350 °C at a heating rate of 10 °C/min. 10–12 mg specimens were cut from each heat treated plaque for DSC analysis. Three specimens were tested for each type of treated samples.

The relative degree of crystallinity (percent improvement in crystallinity compared to as-received sample) ($\eta\%$) values were obtained from Eq. 1 in order to understand the effect of annealing time in water.

$$\eta = (\Delta H_{f,i} - \Delta H_{f,0}) / \Delta H_{f,0} \times 100\% \quad (9)$$

where $\Delta H_{f,0}$ and $\Delta H_{f,i}$ are the heat of fusion of as-received sample and the heat of fusion of sample after the annealing, respectively [19, 20].

As it can be seen from Fig. 6e and Table 3 there is not any notable change on the crystallinity of the samples till 60th day of the annealing process in water. In the other words annealing process does not affect the material before 60th day. The annealing effect shows itself on F-x curves of both $L = 5$ mm and $L = 20$ mm samples (see Fig. 6a, b). From Fig. 6a and b, there is a significant change on the absorbed energy under the area of F-x curves for 60th and 90th day samples both $L = 5$ mm and $L = 20$ mm. 90-20-01 coded sample refers to UHMWPE which is annealed in water for 90 days with ligament length of 20 mm.

SEM images of the fracture surfaces given in Figs. 7 and 8 show the striking effect of the annealing process in water on the fracture response of the material. Fracture surfaces look exactly similar for as-received, 15th day and 30th day samples but after 30th day a remarkable change showed up itself on the fracture surface; a transition from a ductile fracture to a mixed fracture. This transition caused by water uptake of material during annealing process in water. As a result of this transition, EWF parameters as shown in Fig. 6c and d reduced from the 60th day of the annealing process.

Figure 9 shows the effect of annealing process in water on the plastic deformation zone. From this figure it can be seen that there is not any change on the size and shape of the plastic deformation zone till 60th day of annealing process for both $L = 5$ and $L = 20$ mm. This result is parallel to water uptake graphic in Fig. 6e.

Conclusions

The fracture properties of UHMWPE before and after annealing process in water were measured by EWF method as a function of annealing time. From the results presented in this study the following conclusions were drawn:

1. As a result of specimen geometry (SENT) there was no evidence of load-drop at maximum load in any of the F-x curves obtained in this study. UHMWPE did not

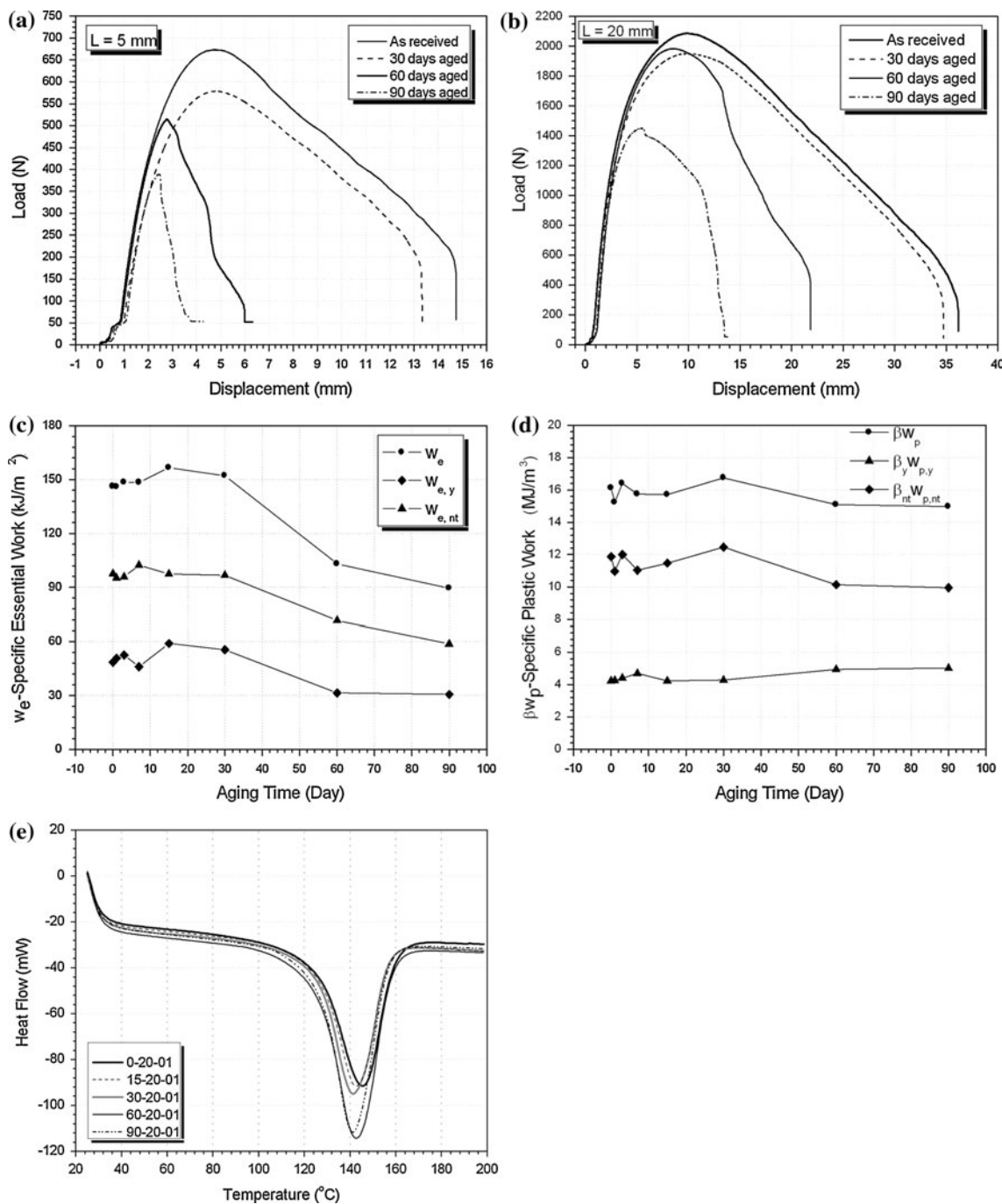


Fig. 6 **a** Load–displacement curves for $L = 5\text{ mm}$ samples as a function of annealing time. **b** Load–displacement curves for $L = 20\text{ mm}$ samples as a function of annealing time. **c** Specific essential work of fracture, w_e and its yielding, $w_{e,y}$ and necking-tearing $w_{e,nt}$ related terms as a function of annealing time for the annealed UHMWPE. **d** Specific plastic work of fracture, w_p and its yielding, $w_{p,y}$ and necking-tearing $w_{p,nt}$ related terms as a function of annealing time for the annealed UHMWPE. **e** Influence of annealing time on the crystallization of UHMWPE

annealed UHMWPE. **d** Specific plastic work of fracture, w_p and its yielding, $w_{p,y}$ and necking-tearing $w_{p,nt}$ related terms as a function of annealing time for the annealed UHMWPE. **e** Influence of annealing time on the crystallization of UHMWPE

- indicate full ligament yielding before the plastic propagation; the EWF method was successfully applied, showing that this requirement does not seem mandatory.
- The results, obtained from water uptake graphic, EWF plots and fracture surfaces show that EWF method was

used properly for UHMWPE before and after annealing process in water.

- Annealing process in water showed up itself neither fracture surfaces nor EWF parameters until 60th day.

Table 3 Relative crystallinity (percent improvement in crystallinity compared to as-received sample) indicators as implied from heat of melting for various annealing times in water

Sample code	ΔH (J g ⁻¹)	η (%)
0-20-01 (as-received)	150.68	0
15-20-01	152.45	1.17
30-20-01	152.69	1.34
60-20-01	157.65	4.62
90-20-01	157.45	4.50

4. Maximum net-section stress elevated at small ligament lengths for as-received material but it did not raise at small ligament lengths for 90th day samples because water acts as plasticizer in material finally plastic deformation zone did not disturbed by lateral boundary of the sample for 90th day samples.
5. The specific EWF terms was more sensitive for the annealing time than the plastic ones.
6. Specific EWF term regressed from (w_e) 146.12 to 89.41 kJ/m² due to annealing effect.

Fig. 7 Effect of annealing time in water on the fracture surface

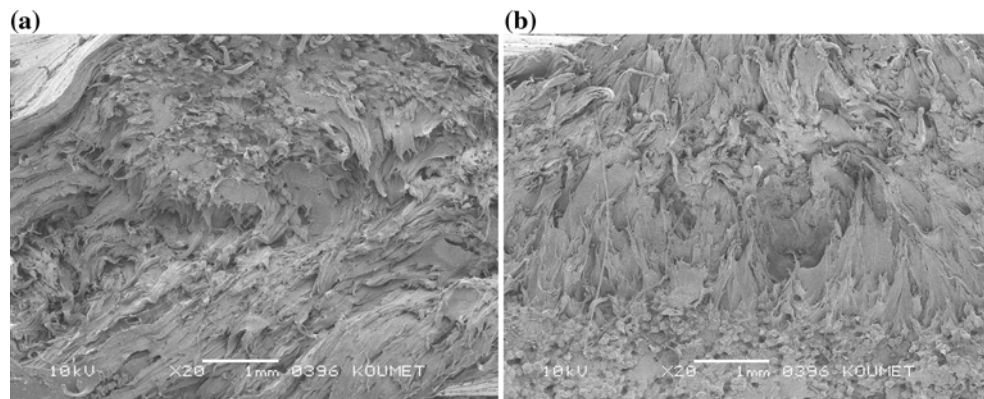
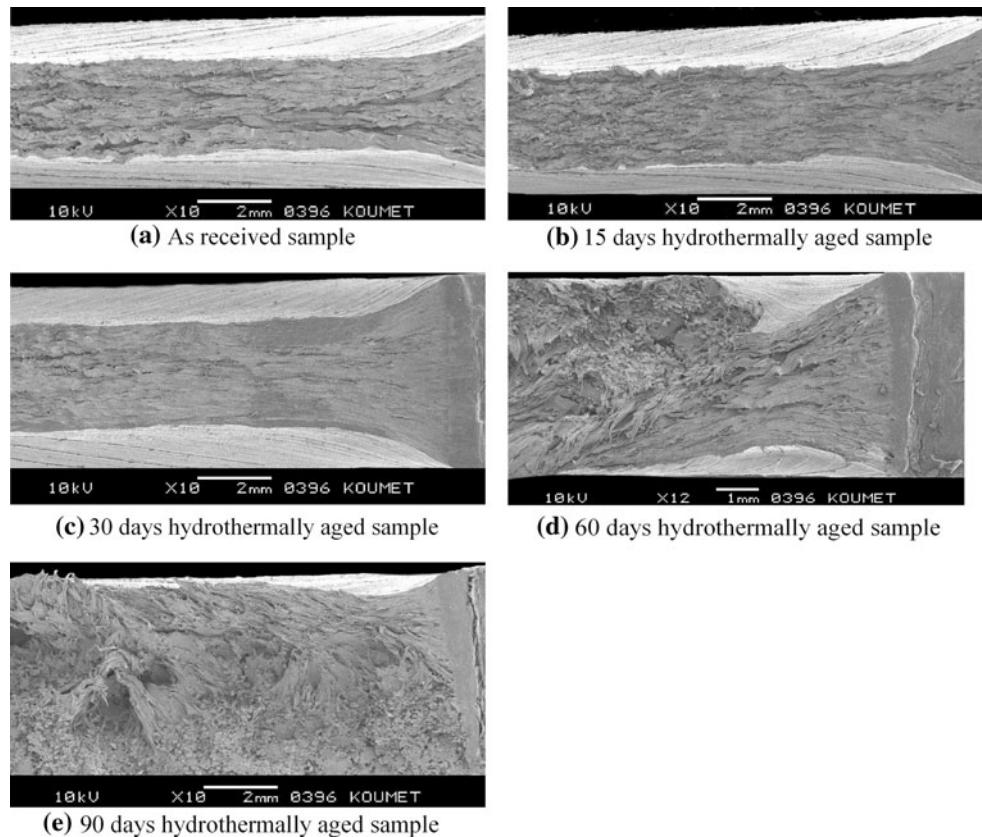


Fig. 8 SEM micrographs of the fracture surfaces of the 60th day and 90th day samples

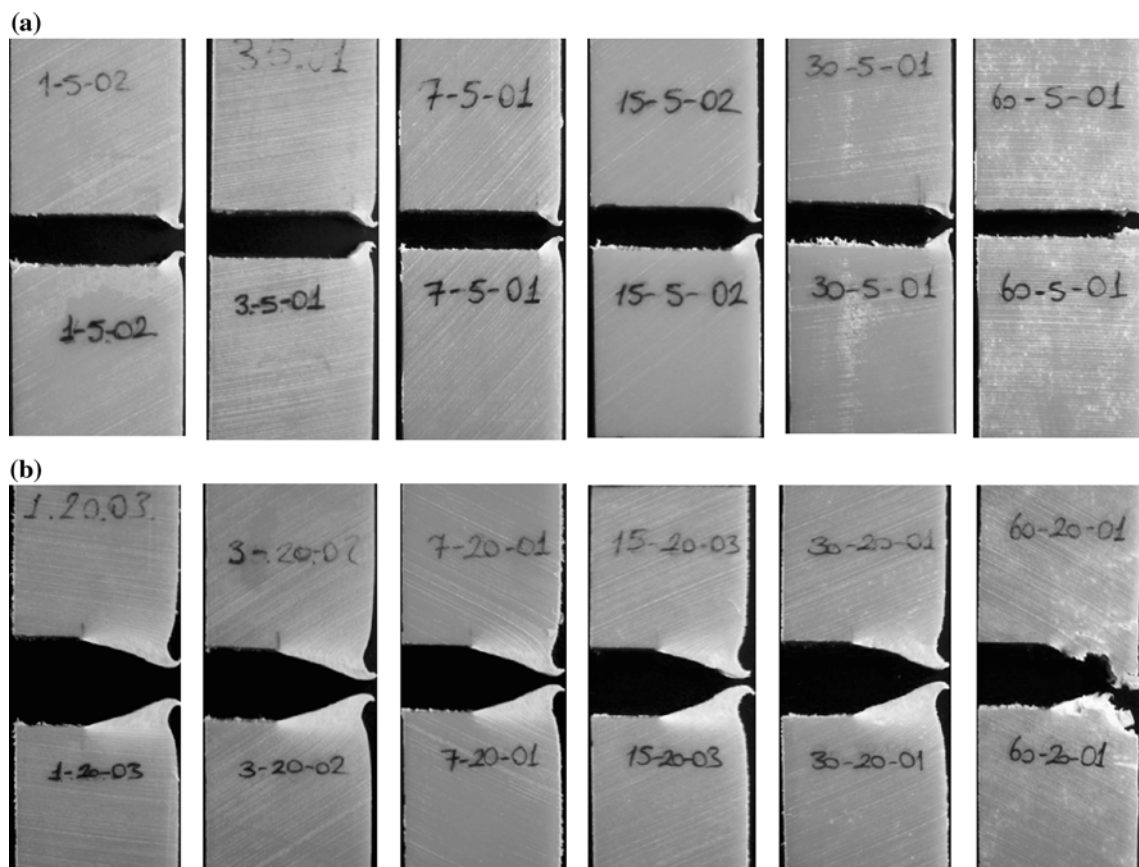


Fig. 9 Effect of annealing time in water on the plastic deformation zone for **a** $L = 5$ mm and **b** $L = 20$ mm samples

References

1. Broberg KB (1968) Int J Fract 4:11
2. Barany T, Karger-Kocsis J, Czigany T (2003) Polym Degrad Stab 82:271
3. Arkhireyeva A, Hashemi S (2001) Polymer 43:289
4. Mouzakis DE, Stricker F, Mülhaupt R, Karger-Kocsis J (1998) J Mater Sci 33:2551. doi:[10.1023/A:1004345017105](https://doi.org/10.1023/A:1004345017105)
5. Hashemi S (2003) J Mater Sci 38:3055. doi:[10.1023/A:1024752508458](https://doi.org/10.1023/A:1024752508458)
6. Mai YW, Cotterell B (1986) Int J Fract 32:105
7. Arkhireyeva A, Hashemi S, O'brien M (1999) J Mater Sci 34:5961. doi:[10.1023/A:1004776627389](https://doi.org/10.1023/A:1004776627389)
8. Arkhireyeva A, Hashemi S (2002) J Mater Sci 37:3675. doi:[10.1023/A:1016561225281](https://doi.org/10.1023/A:1016561225281)
9. Barany T, Ronkay F, Karger-Kocsis J, Czigany T (2005) Int J Fract 135:251
10. Karger-Kocsis J (1996) Polym Bull 37:119
11. Yang W, Xie BH, Shi W, Zuo M, Li ZM, Yang MB (2005) J Mater Sci 40:5323. doi:[10.1007/s10853-005-4398-x](https://doi.org/10.1007/s10853-005-4398-x)
12. Hashemi S (2003) Polym Test 22:589
13. Naz S, Sweeny J, Coates PD (2010) J Mater Sci 45:448. doi:[10.1007/s10853-009-3961-2](https://doi.org/10.1007/s10853-009-3961-2)
14. Chen H, Karger-Kocsis J, Wu J (2004) Polymer 45:6375
15. Barany T, Czigany T, Karger-Kocsis J (2003) Periodica Polytechnica Ser Mech Eng 47:91
16. Karger-Kocsis J, Moskala EJ (2000) Polymer 41:6301
17. Gong G, Xie BH, Yang WY, Li ZM, Zhang WQ, Yang MB (2005) Polym Test 24:410
18. Gong G, Xie BH, Yang W, Li ZM, Lai SM, Yang MB (2006) Polym Test 25:98
19. Yilmaz T (2010) J Mater Sci 45:2381. doi:[10.1007/s10853-009-4204-2](https://doi.org/10.1007/s10853-009-4204-2)
20. Cao J, Chen L (2005) Polym Compos 26:713